The Memoirs of Faculty of Engineering
Fukuyama University
The 17th issue, No.1, Sep., 1993

Scintillation of far-infrared laser beam of wavelength in absorption region

Naoki KAGAWA, Osami WADA*, Ryuji KOGA*, Hiroya SANO

key words: scintillation, far-infrared, PSDF, absorption, anomalous-dispersion

1 Introduction

We are developing a tunable diode laser absorption spectrometry (TDLAS) system, which employs the higher-harmonic detection to monitor green house effect gas concentration.[1] The laser beam whose wavelength is included in 7 μm band scintillates by atmospheric turbulence. The scintillation distorts an absorption spectra and calculated concentration of target gas may suffer from the span error.[2] We try to sweep the spectrum in the time shorter than the autocorrelation time of fluctuation because the air is stable and "frozen" in that short period of time. So it is important for us to know a statistical characteristics of scintillation.

Unlike the visible region, many strong water vapor lines (H_2O) as well as the methane (CH_4) lines share this wavelength region. Water vapor lines exist near methane absorption lines, and interfere methane line in atmosphere where absorption lines are broadened by pressure. It is therefore, considered that characteristics of the scintillation in the absorption band are different from that in visible band where the scintillation is governed solely by the fluctuation in density, not by absorption.

The work on the effect of atmospheric turbulence in an absorption region is due to the complex refractive index as reported by Filho *et al.*.[3] They described the effect of the Oxygen absorption line on the scintillation at 55.5GHz. However, no experimental data of infrared lights have been reported.

In this paper, experimental results of scintillation of 7 μm band laser beam and its theoretical consideration in order to combining Filho's equations and OLP (Optical Line Parameter Compilation) are described.

2 Theoretical background

Scintillation results from temporal and spatial change of refractive index of atmosphere. Temperature, humidity and pressure change cause fluctuation of refractive index. Statistical characteristics of atmospheric turbulence were expressed by Kolmogolov mathematically. Tatarskii solved the scaler Helmholtz's equation, taking the atmospheric turbulence into

* Department of Electrical and Electronic Eng. Okayama University

consideration and obtained spatial power spectral density function (PSDF).[4] This PSDF expressed the scintillation of visible light. Unfortunately, this PSDF can not express the scintillation of electromagnetic wave included in absorption band such as the far infrared. Filho *et al.* calculated the temporal spectrum of scintillation from the spatial spectrum using the Taylor's hypothesis,[3] *viz.*,

$$W_\chi^{\mathrm{L}}(\omega) = 0.85 C_{n\mathrm{R}}^2 \frac{L}{v_\perp} k^2 \left(\frac{L}{k}\right)^{4/3} \left[1+5.15 \frac{C_{n\mathrm{I}}^2}{C_{n\mathrm{R}}^2} \left(\frac{k}{L}\right)^{4/3} \left(\frac{\omega}{v_\perp}\right)^{-8/3}\right] \tag{1}$$

for lower frequency as $f < v_\perp/\sqrt{2\pi\lambda L}$, and

$$W_\chi^{\mathrm{H}}(\omega) = 2.19 \frac{L}{v_\perp} k^2 \left(C_{n\mathrm{R}}^2 + C_{n\mathrm{I}}^2\right) \left(\frac{\omega}{v_\perp}\right)^{-8/3} \tag{2}$$

for higher frequency as $f > v_\perp/\sqrt{2\pi\lambda L}$, where f is temporal frequency in Hz, $v_\perp$ is averaged wind velocity of vertical component and λ is wavelength in meter.

Parameters $C_{n\mathrm{R}}^2[\mathrm{m}^{-2/3}]$ and $C_{n\mathrm{I}}^2[\mathrm{m}^{-2/3}]$ stand for real and imaginary part of refractive index, respectively. They correspond to magnitudes of turbulence of real and imaginary part of the refractive index as

$$C_{n\mathrm{R}}^2 = C_T^2 \left(\frac{\partial n_\mathrm{R}}{\partial T}\right)^2 \tag{3}$$

and

$$C_{n\mathrm{I}}^2 = C_T^2 \left(\frac{\partial n_\mathrm{I}}{\partial T}\right)^2 \quad , \tag{4}$$

respectively. Parameters n_R and n_I are real and imaginary part refractive index, respectively. After Hill's report,[5] each index is shown as

$$n_\mathrm{R} = 1 + \left[N_\mathrm{d} + N_\mathrm{w} + \sum_i N_{ai}\right] \times 10^{-6} \tag{5}$$

and

$$n_\mathrm{I} = \sum_i n_{\mathrm{I}i} \quad , \tag{6}$$

respectively. Parameter N_d shows the contribution of dispersion in dry air:

$$N_\mathrm{d} = 0.3789 \frac{P}{T} \left[64.328 + \frac{29498.1}{146 - (1/\lambda)^2} + \frac{255.4}{41 - (1/\lambda)^2}\right] \quad , \tag{7}$$

where λ is wavelength in μm, P is atmospheric pressure in Torr, and T is atmospheric temperature in Kelvin. The letter N_w shows the contribution of dispersion of water vapor:

$$N_\mathrm{w} = -1.765 \times 10^{-18} Q \quad . \tag{8}$$

Third term in angular brackets of Eq.(5) expresses a contribution of the anomalous-dispersion:

$$N_{ai} = \frac{Q}{4\pi^2 \nu_i} S_i \frac{\nu_i - \nu}{(\nu_i - \nu)^2 + \alpha_i^2} \times 10^6 \quad , \tag{9}$$

where Q is density of water vapor in cm^{-1}/molecules/cm^2, ν_i is center wavenumber of an absorption line and α_i is HWHM of an absorption line.

While n_{Ii} shows the absorption:

$$n_{Ii} = \frac{1}{4\pi^2 \nu} \cdot \frac{QS_i\alpha_i}{(\nu_i - \nu)^2 + \alpha_i^2} \quad . \tag{10}$$

In addition, line strength, S_i, and HWHM of an absorption line, α_i, are shown as

$$S_i = S_{0i} \left(\frac{296}{T}\right)^{1.5} \exp\left[-\frac{E_i^L}{C}\left(\frac{1}{T} - \frac{1}{296}\right)\right] \frac{1 - \exp\left(\frac{-\nu_i}{CT}\right)}{1 - \exp\left(\frac{-\nu_i}{296C}\right)} \quad , \tag{11}$$

$$\alpha_i = b_{Li} \left(\frac{P}{760}\right) \left(\frac{296}{T}\right)^{0.64} \quad , \tag{12}$$

where S_{0i} shows the line strength in 760Torr, 296K. Parameters b_{Li} and E_i^L express HWHM of an absorption line and the lower state energy under the same atmospheric condition. These parameters for all absorption lines are included in the AFGL optical line parameter's data base.[6] Character C is a constant value, 0.695008[$cm^{-1}K^{-1}$].

3 Experiment

Figure 1 shows a schematic diagram of an experimental set up. Two types of diode lasers are employed, one is a PbSnTe tunable diode laser (TDL), 7 μm band, under the test,

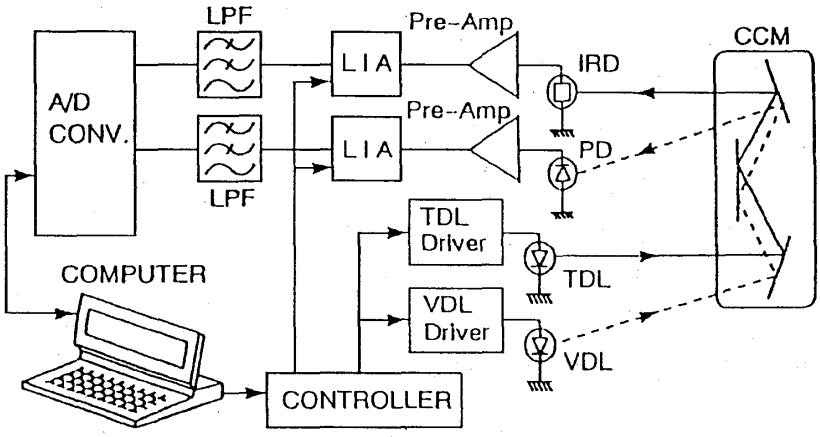

Fig.1 Block diagram of the measurement system: Upper leg is for the tunable diode laser (TDL) and the lower is for the visible diode laser (VDL).

another is visible diode laser (VDL), λ=670nm, in order to measure the atmospheric conditions. Both optical paths of TDL and VDL composed round-trip optical path with a corner cube mirror (CCM) and each of total path length is 140m. Optical paths are rather tilted and elevation from the ground is 7—9m. Laser lights' intensity are modulated electrically, and detected with lock-in amplifiers.

To research an effect of water vapor lines on the scintillation, radiated wavelength is swept over absorption lines. Figure 2 is an transmittance spectrum of TDL. Sixteen wavelengths around water vapor lines are chosen and it is indicated by circle symbols in this figure. Radiated wavelength of TDL is turned by control of injection current. Solid curve in the same figure is calculated with absorption lines' parameters shown in Table 1, those are picked up from OLP (Optical line parameter compilation) published by AFGL (The Air Force Geophysics Laboratory).[5] Center wavelengths are indicated by vertical broken lines in Fig.2. Practically, three particular lines lie in this region though only two lines are appeared clearly in Fig.2. Two lines whose line center are λ=7570.76nm are imposed each other.

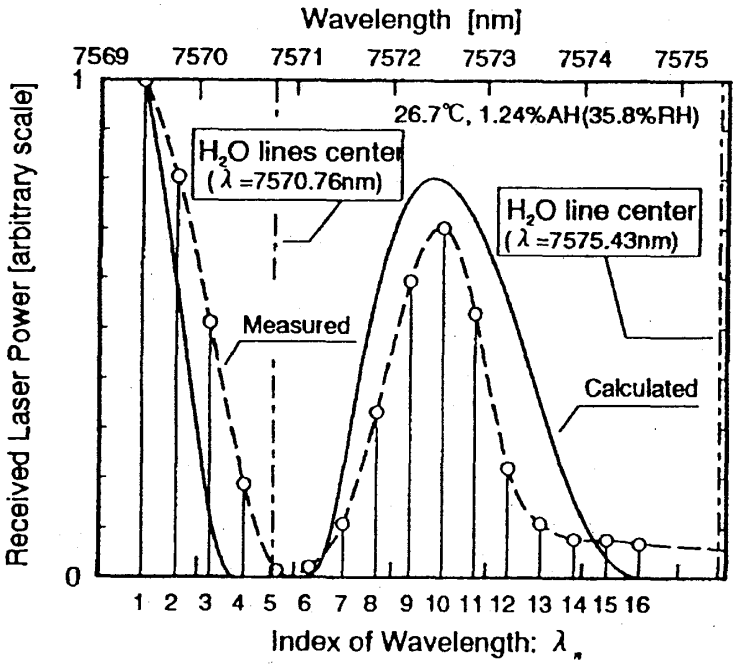

Fig.2 Transmission spectrum of atmosphere around a water vapor lines. Broken line stands for the measured and the solid line for a calculated results. Scintillations were measured on the 16 wavelengths indicated with vertical solid lines in this figure.

Table.1 Line-parameters of water vapor.

Line center [nm]	7570.76	7570.76	7575.43
Line intensity at 296K : S_{0i} ($\times 10^{-22}$) $cm^{-1}/(molecule \cdot cm^{-2})$	2.180	6.540	14.4
Half width at 760Torr : b_{Li} $cm^{-1}/760Torr$	0.0282	0.0278	0.0861
Lower state energy : E_i^L [cm^{-1}]	1789.041	1789.041	602.774

4 Results

Figure 3 shows experimental and theoretical PSDF of four radiated wavelength, which are λ =7569.44nm, 7570.13nm, 7570.82nm and 7571.16nm. Experimental results are indicated by four types of symbols and the theoretical results calculated by Eq.(1) and (2) are indicated by different types of lines. As shown in Fig.2, strong water vapor lines whose center wavelength is λ =7570nm exist and λ_5(λ =7570.82nm) is the closest wavelength for these water vapor lines. Inspecting Fig.3, profiles of experimental results will be similar each other in higher frequency region. Unfortunately, the higher frequency region of λ_5 and λ_6 are hidden by electric noise because received laser power is reduced by absorption of water vapor lines. Profiles and the higher corner frequency of PSDF are the same on the theoretical curves, and the slope is −8/3. While, in lower frequency region less than 1Hz, spectrum level of λ_5, cross symbols and λ_6, circle, especially λ_5, are enhanced and these phenomenon can not be found in the others. Inspecting the theoretical results, it is found that the level enhancement is not extinct but sifts to lower frequency when the radiated light's wavelength separates from the central wavelength of the absorption line. So, the lower corner frequency of λ_1 and λ_3 may disappear from measurable frequency range of our system.

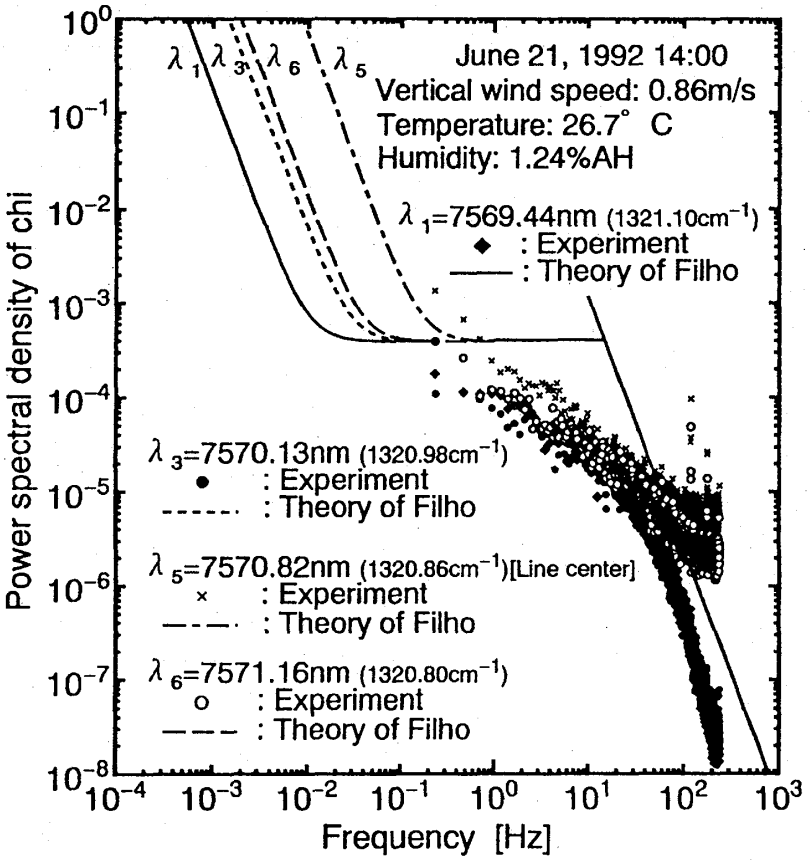

Fig.3 Power spectral density function of log amplitude obtained at 14:00 on June 21, 1992.

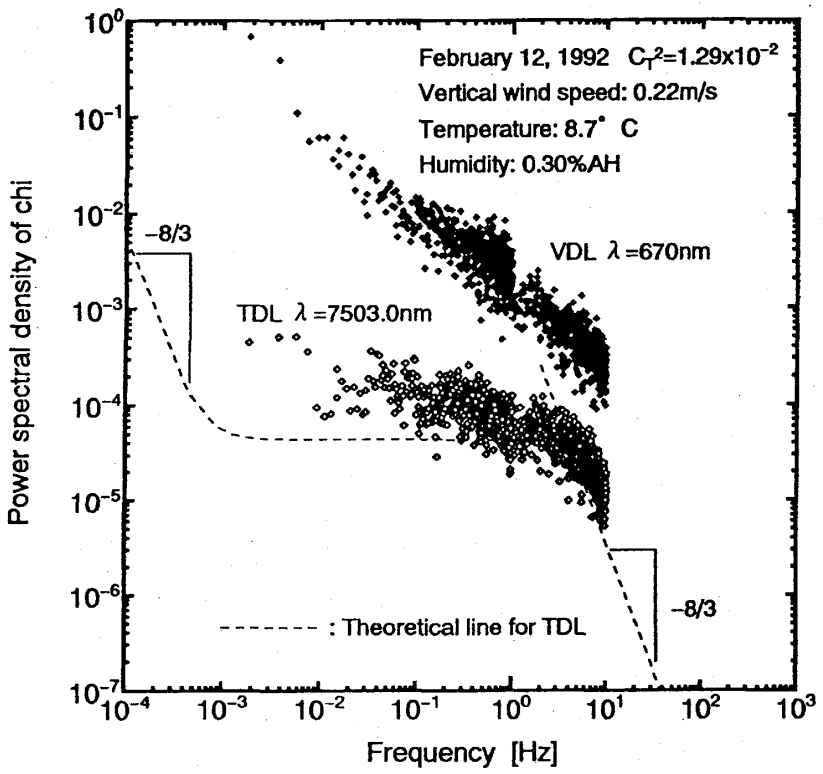

Fig.4 The lower frequency region of power spectral density measured in winter. TDL wavenumber was fixed on 7503.0nm, which was just on a water vapor line.

Similar experiments were repeated under different climates to investigate PSDF in lower frequency region than previous experiment. Data for the lower frequency regions, from 10^{-3}Hz to 1Hz, and those for the middle region, from 10^{-2}Hz to 10Hz, are taken separately because of our system band-width and are shown on the same figure. Records of data of Fig.4 and Fig.5 are measured in winter, and Fig.6 in summer. Profile of the spectrum for VDL resembles each other and the levels are also the same in winter. Spectra for TDL of Figs.5 and 6 are enhanced at lower frequency that were less than 10^{-2}Hz, however it is not found in Fig.4. Theoretical lines calculated by Eqs.(1), (2) were drawn in the same figures of experimental results. Theoretical curves agree well with experimental data and it was found that the lower corner frequency of the experimental data of Fig.4 is below the measurable frequency range. Therefore, the spectral level of Fig.4 was expected to enhance in much lower frequency region less than 10^{-3}Hz. The level of the spectrum of the TDL in summer is approximately 10 times bigger than that in winter, and comes down to that of VDL. This result means that the level of power spectral density is governed by humidity at around a spectral region near water vapor lines, because this level may be decided by anomalous dispersion.

The lowest two traces of Fig. 6 are the laser power fluctuation spectra of the infrared TDL and VDL. The spectrum for VDL is enhanced at lower frequency that is less than 0.01Hz, which is not attributed to atmospheric turbulence. Fluctuation in the VDL output is too weak to govern this phenomena as shown also in Fig.6. Full explanation has not been found. On the other hand, the slope of the laser power fluctuation spectrum for TDL is approximately -1 and is not as steep as that of 140m path at lower than 0.03Hz. Thus, the

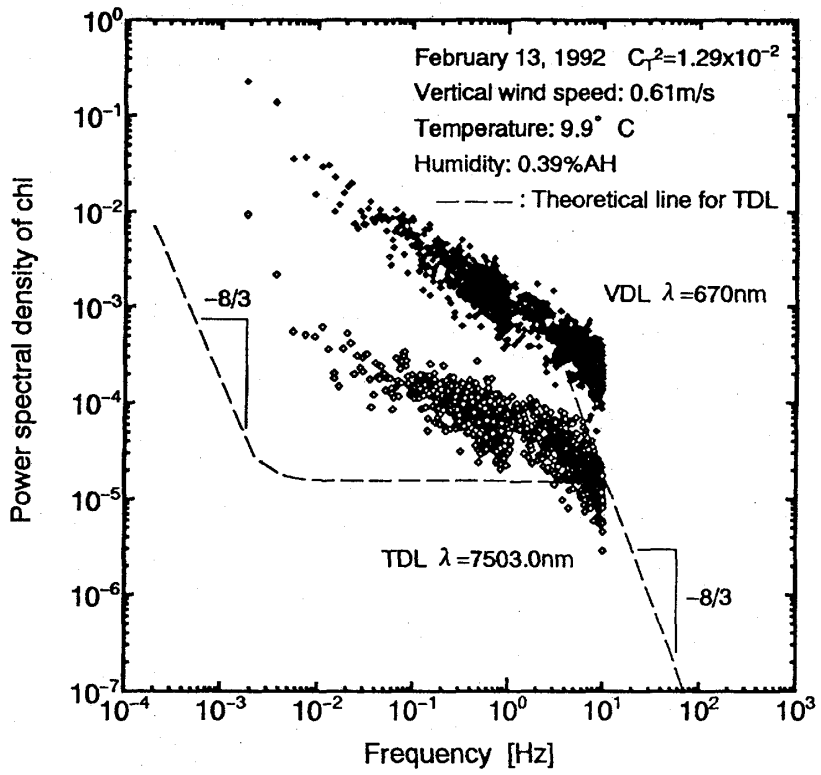

Fig.5 Results of the similar experiments have been done in another winter daytime. The level of spectral density function rose in the lower frequency region less than 10^{-2}Hz.

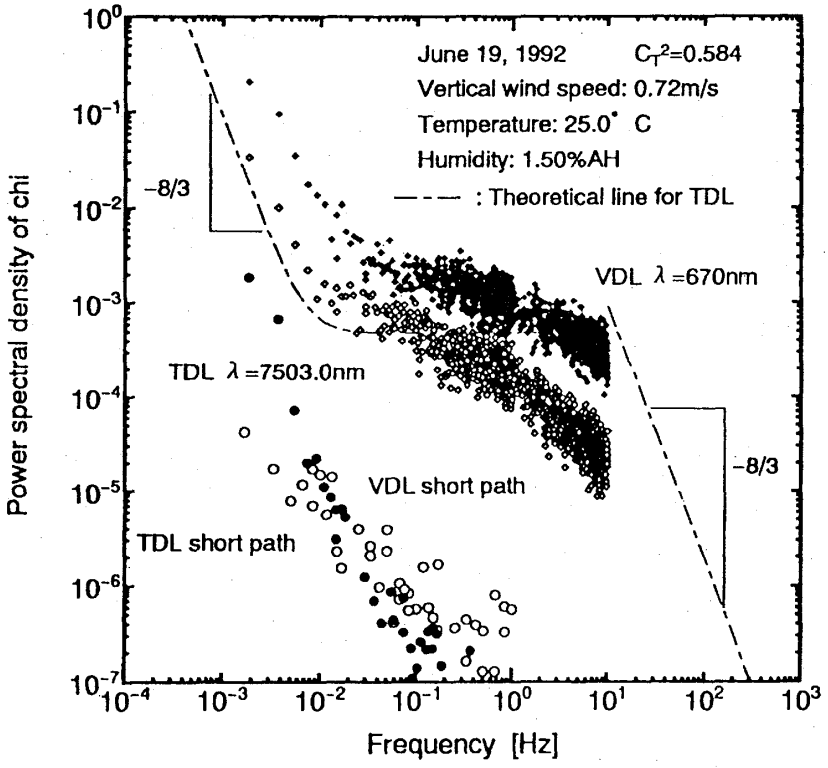

Fig.6 Results of the similar experiments have been done in summer. The level enhancement appeared in particular in lower frequency region less than 10^{-2}Hz. A power spectral density function of log amplitude of the aser emission power is also shown.

lower frequency enhancement of the PSDF for infrared TDL should be due to water vapor absorption. Filho claims that the absorption contributes to the steep slope of −8/3 in lower frequency and our spectra of TDL are found similar to his result.

5 Conclusion

The fluctuation of the log−amplitudes of the PSDF in the atmosphere for 7 μm band infrared light was experimentally found to be enhanced in the frequency region less than 0.03Hz. We found that both the water vapor absorption lines affect the PSDF of log−amplitude fluctuation in the lower frequency region as 55.5GHz millimeter wave is affected by the Oxygen absorption line. Moreover, present experiment gave the cut−off frequency of the scintillation for infrared light. This result is useful in our attempt to determine the period in which obtain the absorption spectrum of the scintillation could be "frozen" with our LAS system.

Acknowledgement

The authors express sincere thanks to students of Okayama Univ., Koga Lab., who cooperated in the preparation and measurements. Special thanks are extended to Fujitsu Laboratories Inc., who supplied us with laser diode of the best quality, that can not be found elsewhere in the world.

References

[1] N.Kagawa, O.Wada, H.Xu, R.Koga, H.Sano and K.Inubushi: "*In Situ* and Real−Time Measurement of Methane Concentration in Rice Paddy Field at Okayama University Using Tunable Diode Laser Absorption Spectrometry", *Japan J. Appl. Phys.*, **32**(1992) pp.244−245.

[2] N.Kagawa, R.Koga, O.Wada and H.Sano: "Measurement of Scintillation for a Horizontal Beam in 7 μm Range", *IEICE Tech. Rep.*, **OQE91−151**(1991) pp.1−6(in Japanese).

[3] F.C.Medeiros Filho, D.A.R.Jayasuriya, R.S.Cole and C.G.Helmis: "Spectral Density of Millimeter Wave Amplitude Scintillations in an Absorption Region", *IEEE Trans. Antennas and Propagation*, **AP−31**(1983) pp.672−676.

[4] V.I.Tatarskii: "The effect of the turbulent atmosphere on wave propagation", *Israel Program for Scientific Translation Ltd., Jerusalem*, Chap.4(1971) pp.259−334.

[5] L.S.Rothman, R.R.Gamache, A.Goldman, L.R.Brown, R.A.Toth, H.M.Pickett, R.L.Poynter, J.−M.Flaud, C.Camy−Peyret, A.Barbe, N.Husson, C.P.Rinsland and M.A.H.Smith: "The HITRAN database: 1986 edition", *Appl. Opt.*, **26**(1987) pp.4058−4097.